International Journal of Food Microbiology 441 (2025) 111301

Contents lists available at ScienceDirect

International Journal of Food Microbiology

journal homepage: www.elsevier.com/locate/ijfoodmicro

Detection of *Fusarium* spp. and T-2 and HT-2 toxins contamination in oats using visible and near-infrared spectroscopy

Irene Teixido-Orries [a], Lexuan Yang [b], Francisco Molino [a], Angel Medina [b], Sonia Marín [a], Carol Verheecke-Vaessen [b,*]

[a] Applied Mycology Unit, Department of Food Technology, Engineering and Science, University of Lleida, AGROTECNIO-CERCA Centre, Av. Rovira Roure 191, 25198 Lleida, Spain

[b] Magan Centre of Applied Mycology, Cranfield University, Cranfield MK43 0AL, United Kingdom

ARTICLE INFO

Keywords:
Applied mycology
Oat
Fusarium langsethiae
Vis-NIR spectroscopy
HT-2 toxin
T-2 toxin
Mycotoxin detection
Fungal contamination

ABSTRACT

Fusarium langsethiae (FL) is one of the major contaminants in oats in the United Kingdom (UK) and is a significant producer of T-2 and HT-2 toxins, among the most prevalent mycotoxins in oats. Visible and near-infrared (Vis-NIR) (350–2500 nm) spectroscopy was explored as a non-invasive, rapid method for detecting FL, *Fusarium* species that produce T-2 and HT-2 toxins, and T-2 and HT-2 toxins content. Oat grains were artificially inoculated with FL and other *Fusarium* species under controlled water activity (a_w) conditions (0.98, 0.90, and 0.80). FL was found to be particularly responsible for producing T-2 and HT-2 toxins. Classification models were developed to distinguish oat grains based on the presence of FL. The best performance was achieved with all the Vis-NIR spectra, with a classification accuracy of 76.2 %. The Vis region (350–995 nm) emerged as the most important range for classification. Additionally, oat grains were classified by T-2 and HT-2 toxin content, distinguishing oats above and below the European Union (EU) threshold with 93.3 % accuracy. For mycotoxin quantification, the best performance was obtained using the Vis region with a coefficient of determination (R^2) of 0.875. Key wavelengths such as 464, 568, 575 and 636 nm were relevant for toxin detection. The NIR region (1005–1795 nm) also played a significant role in the models. This study shows that Vis-NIR spectroscopy is a promising, non-destructive tool for detecting *Fusarium* and type A trichothecenes in oats, though further research is needed to improve model robustness and support food safety monitoring.

1. Introduction

Oats are increasingly recognised for their health benefits, particularly their positive impact on cardiovascular health (Thies et al., 2014), as well as for their functional food properties, which have contributed to their rising popularity in contemporary diets (Rasane et al., 2015). For example, 830 k tonnes of oats were produced in 2023 in the United Kingdom (UK), representing approximately £157M annum (FAOSTAT, 2023). However, in the UK, *Fusarium* spp. can contaminate up to 66 % of oat crops, often leading to the accumulation of mycotoxins which pose significant food safety risks (Xue et al., 2019).

In oats, *Fusarium* spp. act as symptomless phytopathogens, infecting the crop without producing visible signs of disease (Tekauz et al., 2008). The predominant *Fusarium* species associated with oats include *F. poae* (FP), *F. graminearum* (FG), *F. langsethiae* (FL), *F. sporotrichioides* (FS), *F. avenaceum*, and *F. culmorum* (Gil-Serna et al., 2022; Islam et al., 2021), although their distribution varies depending on the region of oats production. As above-mentioned, these *Fusarium* infections can lead to different production of mycotoxins, such as type A and B trichothecenes and zearalenone (ZEN), which are regulated by the European Union (EU). These mycotoxins could seriously affect human and animal health (Marin et al., 2013). In consequence, EU regulatory limits have been established for several mycotoxins in unprocessed oats. These include: (i) deoxynivalenol (DON, a type B trichothecene) with a maximum permitted level of 1750 μg/kg; (ii) ZEN at 100 μg/kg; and (iii) the type A trichothecenes T-2 and HT-2 toxins, with a combined maximum level of 1250 μg/kg (European Commission, 2024a, 2024b, 2023). In addition to these regulated compounds, several other mycotoxins have been detected in oats, such as nivalenol (NIV) (Fredlund et al., 2013; Perkowski et al., 2012; Teixido-Orries et al., 2025a). Of particular concern, T-2 toxin is regarded as the most toxic trichothecene mycotoxin, as it has several harmful effects on humans and animals on the cardio-cerebrovascular system, central nervous system, gastrointestinal tract,

* Corresponding author.
E-mail address: c.verheecke@cranfield.ac.uk (C. Verheecke-Vaessen).

https://doi.org/10.1016/j.ijfoodmicro.2025.111301
Received 1 April 2025; Received in revised form 22 May 2025; Accepted 2 June 2025
Available online 4 June 2025
0168-1605/© 2025 The Authors. Published by Elsevier B.V. This is an open access article under the CC BY license (http://creativecommons.org/licenses/by/4.0/).

Nomenclature

a_w	Water activity
DON	Deoxynivalenol
DSS	Decision Support Systems
EU	European Union
FL	*Fusarium langsethiae*
FG	*Fusarium graminearum*
FP	*Fusarium poae*
FS	*Fusarium sporotrichioides*
kNN	k-Nearest Neighbours
LC-MS/MS	Liquid Chromatography-Tandem Mass Spectrometry
LDA	Linear Discriminant Analysis
NIR	Near-Infrared Range
NIR-HSI	Near-Infrared Hyperspectral Imaging
NIV	Nivalenol
PC	Principal Components
PCA	Principal Component Analysis
PDA	Potato Dextrose Agar
PLS	Partial Least Squares
R^2	Coefficient of determination
RMSECV	Root Mean Square Error of Cross-Validation
RPD	Ratio of Per cent Deviation
SECV	Standard Error of Cross-Validation
SNV	Standard Normal Variate
UK	United Kingdom
Vis	Visible range
Vis-NIR	Visible and Near-Infrared Range

skin and other important organs (Janik et al., 2021). HT-2 toxin is as toxic as T-2 toxin, as T-2 is rapidly metabolised into HT-2 following animal ingestion (Pettersson, 2011). Notably, the highest levels of T-2 and HT-2 toxins contamination in oats have been reported in the UK, Ireland, and Switzerland (De Colli et al., 2021; Kolawole et al., 2021; Verheecke-Vaessen et al., 2019), where production of these toxins has primarily been attributed to FL (Edwards, 2009; Luo et al., 2021).

Although several decision support systems (DSS) are available for monitoring mycotoxin contamination in wheat and barley under field conditions (Rossi et al., 2007), there remains a notable lack of tools specifically tailored to oats. This gap in detection infrastructure increases the likelihood of contamination going unnoticed, resulting in elevated levels of mycotoxins in oat-derived products. In fact, studies have shown that up to 17 % of oat samples have exceeded the former EU indicative levels for T-2 and HT-2 toxins (1000 μg/kg) (European Commission, 2013), posing significant health concerns and economic losses (Xue et al., 2019). Compounding the issue, research indicates that while most oat grains in a batch are typically free of mycotoxins, a small subset may carry disproportionately high toxin loads, ultimately driving the overall contamination level of the batch. The presence of even a few highly contaminated grains can compromise the safety of the entire lot (Teixido-Orries et al., 2025a).

To address this challenge, early detection and removal of contaminated grains is crucial, ideally as soon as possible in the supply chain. The timely removal of highly contaminated grains can significantly reduce the transfer of mycotoxins from raw material to the final oat-based products, thereby preserving the safety and quality (Dropa et al., 2021; Teixido-Orries et al., 2025b; Tittlemier et al., 2020). However, visual inspection by humans is not a viable approach due to the typically asymptomatic nature of *Fusarium* infection and mycotoxin production in oats. In this context, spectroscopy-based sorting emerges as a promising solution: it is automated, non-destructive, and cost-effective, making it well-suited for real-time detection and removal of contaminated grains.

Spectroscopic techniques have gained considerable attention as rapid tools for both the semi-quantification of mycotoxins and the detection of fungal damage in cereals such as wheat, barley, maize, and oats (Femenias et al., 2020). The effectiveness of these techniques largely depends on the spectral range used. The visible (Vis, 400–700 nm) region is particularly useful for detecting physical traits such as discolouration and structural damage, while the near-infrared (NIR, 700–2500 nm) region is more suitable for assessing chemical composition and moisture levels (Walsh et al., 2020). Notably, a subtle darkening effect has been observed in oat grains contaminated with DON, which may act as a detectable marker in the Vis range (Tekle et al., 2013). Therefore, combining Vis and NIR spectroscopy can enhance analytical performance (Walsh et al., 2020).

Recent studies have demonstrated the potential of Vis-NIR spectroscopy for estimating DON concentrations in artificially contaminated ground oats with promising accuracy (Tekle et al., 2013). Furthermore, near-infrared hyperspectral imaging (NIR-HSI) has been shown to be effective in detecting FG-infected oats (Tekle et al., 2015), and in classifying naturally contaminated oat samples according to their DON, and T-2 and HT-2 toxins level (Teixido-Orries et al., 2023b, 2023a). Despite these advances, to date there is no published research on the application of Vis-NIR spectroscopy for the detection of FL or for identifying T-2 and HT-2 toxins contamination at the level of individual oat grains.

Given these gaps in current monitoring tools and the potential of spectral technology, this study aimed to evaluate the potential of Vis-NIR spectroscopy for classifying oats based on: (1) the presence or absence of *Fusarium* species capable of producing T-2 and HT-2 toxins; (2) the specific presence of FL; and (3) the classification of oats according to the EU legal limit for T-2 and HT-2 toxins. Additionally, this study sought to identify key Vis-NIR spectral regions and wavelengths for prediction and to assess the influence of water activity (a_w) on fungal growth and mycotoxin production in oats.

2. Materials and methods

2.1. Materials

All mycotoxin standards were supplied by Romer Lab (Tulln, Austria) and were dissolved in acetonitrile. These include DON (100 μg/mL), NIV (100 μg/mL), HT-2 toxin (100 μg/mL) and T-2 toxin (100 μg/mL).

Ultrapure water was obtained with PURELAB® Chorus 1 (ELGA LabWater; Buckinghamshire, UK). Ammonium acetate (>99 %, analytical reagent grade), acetic acid glacial (99.7 %, HPLC grade), acetonitrile (LC-MS grade), methanol (LC-MS grade), formic acid (LC-MS grade), glycerol (>99 %), V8 media, and isopropanol (analytical reagent grade) were obtained from Fisher Scientific (Waltham, MA, USA). Tween 80 (Sigma-Aldrich; St. Louis, MO, USA) and Potato Dextrose Agar (PDA) (Oxoid; Hampshire, UK) were also used in the preparation and culturing of fungal strains for the experiments.

2.2. Fungal strains

The fungal strains used in this study included FL 2391 (strain 1), FL GFP VI 06063 (strain 2), FS 202,176, FG 08/111, and FP 202,172. The strains were cultivated for 8 days on PDA medium, except for FG 08/111, which was grown on V8 medium, at 25 °C. Spore suspensions were prepared by harvesting spores in sterile water supplemented with 0.005 % Tween 80. FL2, FS and FP strains are from the collection of the Norwegian Institute of Bioeconomy Research, and they are originally from Norway. FL1 is from the collection of Food and Environment

Research Agency in the UK, and it is originally from the UK. FG is from the collection of Harper Adams University, and it is also originally from the UK. All the strains were isolated from oat grains.

2.3. Oats water activity adjustment

Oats harvested in the UK were collected and irradiated at 12–15 kGys gamma irradiation (SynergyHaelth Ltd., Swindon, UK). A moisture adsorption curve was developed and used to accurately add known amounts of sterile water to sub-samples of the oats to obtain the target a_w levels of 0.98 (optimum production of mycotoxin production by the *Fusarium* tested), 0.90 (permissive condition for growth, but boundary in terms of mycotoxin production) and 0.80 (control outside of the permissive a_w for *Fusarium* growth). To equilibrate the moisture content, the oats were kept in sealed containers at 4 °C for 48 h and shaken twice a day to allow adsorption and equilibration.

2.4. Inoculation and incubation conditions

The different fungal strains suspensions were adjusted to get a final concentration of 10^3 spores per gram after oats inoculation. Oat grains were placed in 80-mL jars inside airtight containers, along with a beaker containing a glycerol/water solution (30:70, *v/v*) to maintain the desired a_w. The oat grains were incubated for 10 days at 25 °C.

Table 1 presents the sample group settings, with different fungal strains inoculated at three water activity levels (a_w = 0.80, 0.90, and 0.98). Each a_w/strain condition was tested in triplicate. The control oat samples were preliminary tested for mycotoxin concentration, however, given the un-even distribution of mycotoxin in oats, control samples may still exhibit spots of mycotoxin contamination.

2.5. Spectra measurement

For each replicate, 35 oat grains were randomly selected. Each replicate consisted of 35 oat grains, selected to simulate a worst-case contamination scenario where only a small proportion of grains within a batch may be infected. This number also provided a practical compromise between experimental manageability and capturing representative variability. Spectral data were collected from these individual grains per a_w/strain condition, resulting in a total of 2100 spectra, calculated as follows: (2 a_w × 7 inoculated fungi) + (1 a_w × 6 inoculated fungi) × 3 a_w/strain replicates × 35 grains.

A LabSpec 2500® Near-Infrared Analyzer (350–2500 nm; Analytical Spectral Devices Inc., USA) was used for spectral acquisition. The system included three detectors: one silicon array (350–1000 nm) and two Peltier-cooled InGaAs detectors (1000–1800 nm and 1800–2500 nm), with a sampling interval of 1 nm. Oat grains were placed in direct contact with a fibreoptic cable connected to an in-built quartz-halogen light source (Ocean Optics, USA), and spectra were recorded in reflectance mode. To reduce external light interference, a sample tray and a black bottle cap were used.

To ensure measurement accuracy, the system was turned on 50 min before data collection. A Spectralon® Diffuse Reflectance Standard was used for calibration before starting the measurements, between different sample groups, and after every ten grains. Additionally, a baseline was recorded, and three preliminary spectra were taken to confirm system stability before proceeding with the full dataset.

Table 1
Sample group setting. *Fusarium langsethiae* (FL); *Fusarium sporotrichioides* (FS); *Fusarium graminearum* (FG); *Fusarium poae* (FP).

a_w	Fungi inoculated						
0.80	None (Control)	FL1	FL2	FS	FG	FP	–
0.90	None (Control)	FL1	FL2	FS	FG	FP	FL2 + FP
0.98	None (Control)	FL1	FL2	FS	FG	FP	FL2 + FP

Between different groups, the workspace was disinfected with a 70 % isopropanol solution to prevent cross-contamination. The spectroscopy system included the LabSpec analyzer, an interactance probe connected to the light source, and a computer running Indico Pro image acquisition software (Malvern Panalytical Ltd., Malvern, UK).

After spectral acquisition, the T-2 and HT-2 toxins content in oats from each replicate was analysed using liquid chromatography-tandem mass spectrometry (LC-MS/MS).

2.6. LC-MS/MS analysis: determination of mycotoxins' content

The same 35 oat grains of each replicate used in Section 2.5 were grounded in a Waring Laboratory & Science homogeniser model 7009G (Waring Laboratory Science, CT, USA) during 5 min at maximum speed. The samples were stored at 4 °C until analysis. After homogenization, 100 ± 10 mg of oat material were weighed into 2 mL Eppendorf tubes and extracted with 500 μL of acetonitrile:water:formic acid (79:20.9:0.1, *v/v/v*) for 90 min with 300 rpm at 25 °C on a rotary shaker (miniShaker VWR, Leighton Buzzard, UK). Afterward, the extracts were centrifuged for 10 min at 22,600 ×*g* (Centrifuge 5417S Eppendorf, Stevenage, UK). The supernatants (200 μL) were transferred to vials containing 250 μL microinserts and kept at −20 °C until appropriate shaking before analysis.

For LC-MS/MS analysis, measurements were performed with an Exion series ultrahigh performance liquid chromatography system coupled to 6500+ qTRAP-MS system coupled with IonDriveTM Turbo Spray (both Sciex Technologies, Warrington, UK). Chromatographic separation was achieved on a reversed-phase ACE 3-C18 column (2.1 × 100 mm, 3 μm particle size; Hichrom) equipped with a C18 security guard cartridge (4 × 3 mm, Gemini, Agilent) kept at 40 °C. The gradient elution was carried out with water:acetic acid (99:1, *v:v*) (solvent A) and methanol:acetic acid (*v:v*, 99:1) (solvent B), both supplemented with 5 mM ammonium acetate to promote the formation of ammonium adducts. The applied gradient was 15 min long as described: 0 min, 10 % B; 0–2.0 min, 10–40 % B; 2.0–10.0 min, 100 % B; 10.0–11.50 min, 100 % B; 11.50–12.0 min, 5 % B; 12.00–15.0 min, 5 % B. The flow rate of the mobile phase was 0.3 mL/min, and the injection volume was set to 3 μL.

ESI-MS/MS was performed in unscheduled Multiple Reaction Monitoring (MRM) mode in positive and negative mode with a dwell time of 10 msec per Q3 analysed (Table S1). The source conditions were set as follows: Curtain gas 40 %, Collision Gas Medium, IonSpray voltage −4500 V (in negative) and 5500 V (in positive), Temperature 400 °C, ion source gas 1 60 psi and ion source gas 2 60 psi, the Entrance Potential for all compound was fixed at 10 V. The acquisition of 2 MRM per analyte were analysed to confirm identity of the identified metabolite. Data were acquired with Analyst® Data Acquisition version 1.6.3, and quantification of data was performed using MultiQuant™ version 3.0.3.

To assess the performance of the method, oat samples were weighed 100 ± 10 mg in replicates (n = 8) and were spiked with a solution containing all target analytes in acetonitrile on five levels (500, 250, 100, 50, 10 μg/kg). The samples were vortexed and gently spined down for 10 s before storage overnight at room temperature to ensure solvent evaporation and to achieve equilibrium between the analytes and the matrix. The next day, the samples were extracted according to the procedure described above. 4 replicates out of 8 were spiked after extraction to match the oat toxins concentration. The peaks were integrated and linear 1/× weighted, calibration curves were constructed from the data obtained from the analysis. The S/N ratios were assessed at the lowest reliably visible spiked oats and the limit of detection (LOD) and the limit of quantification (LOQ) were calculated based on Malachová et al. (2014).

2.7. Spectral data analysis

First, to analyse the data, a spectral comparison was developed using Quasar (version 1.5.0, University of Ljubljana, Slovenia) based on

Orange 3.0 created by Toplak et al. (2021). We calculated the mean spectra for each a_w/strain condition and each fungal species. Spectra were labelled by a_w/strain condition, and the presence of *Fusarium* T-2 and HT-2 toxins producers and non-producers.

Then, the spectral data were pre-processed by the application of different spectral modifications also by Quasar software (version 1.5.0) to correct the data and avoid some spectroscopic effects. The two pre-treatments applied to transform raw data were the first derivative (Savitzky-Golay Filter: window 5, polynomial order 2, derivative order 1) and Standard Normal Variate (SNV). Principal Component Analysis (PCA) projections were performed on the mean spectra without and with spectral data pre-processing. PCA aimed to identify general trends and highlight valuable information from the spectral data. For this reason, PCA was executed by type of fungi and a_w using all a_w conditions. Moreover, PCA analysis was also developed to observe trends about the presence of FL and the presence of *Fusarium* T-2 and HT-2 toxins producers but only using 0.98 and 0.90 a_w conditions.

Prediction models were built by the mean spectra of twenty different a_w/strain conditions (three replicates per condition) using Unscrambler software (version 7.6 SR1, CAMP, Oslo, Norway, 2001). Mean spectra were considered as explanatory variables and T-2 and HT-2 toxins content as the dependent variable. A total of sixty mean ($n = 35$) spectra were obtained to develop cross-validated Partial Least Squares (PLS) models. PLS regressions were developed with raw spectra and with pre-processed spectra with the first derivative and SNV that we also applied in the PCA. Moreover, the models were performed using the whole spectra (350–2500 nm), the Vis region (350–995 nm) (although it includes some of the near-NIR), the NIR region 1 (1005–1795 nm) and the NIR region 2 (1805–2500 nm), so twelve PLS models were obtained.

For the depuration of the data, data points which differed significantly from the other samples were considered outliers. The criteria followed for outlier exclusion was to represent the residual influence plot, which represented the residual Y variance versus the leverage. Outliers that presented high values of both parameters were removed. A maximum percentage of 5 % of mean spectra was removed.

In addition, to enhance the models and to avoid scattering effects, initial extremes of the spectra were also subtracted, and in consequence, the 351–413 nm region was eliminated in the Vis region and whole spectra models.

Full cross-validation (leave-one-out) was used in these models, as this is the most suitable type of validation for small and non-balanced data sets and with a narrow range. The criteria used to select the number of optimal principal components (PC) was the PC number where the first minimum on the root mean square error of cross-validation (RMSECV) occurred. The performance parameters that determined the fitness of the models consisted of the slope, offset, RMSECV, correlation, coefficient of determination (R^2), square error of cross-validation (SECV), number of PC and ratio of per cent deviation (RPD). The RPD is a ratio between the standard deviation of the laboratory-measured data and the RMSECV, and it is a useful metric for evaluating the performance of the models. An RPD >2.5 indicates excellent predictions, 2.0–2.5 suggests good predictions, and values between 1.4 and 1.8 indicate that the model can distinguish high and low values, but with less precision (Agelet and Hurburgh, 2010). The best-fitted models were selected following the combination of the closest to 1 for slope and correlation and R^2, the highest RPD and the lowest RMSECV, SECV, offset and number of PC.

Finally, characteristic wavelength for the best-adjusted models (the spectral band with the highest weight on the models and that contributed substantially to explaining T-2 and HT-2 toxins variance) were selected by the highest absolute value of regression coefficient in the regression coefficient representation.

Classification models according to the presence of FL, the presence of *Fusarium* T-2 and HT-2 toxins producers and the content of T-2 and HT-2 toxins were developed based on the spectral information. The models built were: Neural Network, k-Nearest Neighbours (kNN) and Linear Discriminant Analysis (LDA). Neural Network (100 neurons in hidden layers; ReLu activation; Adam Solver; 200 maximal number of iterations; regularization $\alpha = 0.0001$) and kNN (number of neighbours 5; Euclidean metric, Uniform weight) were also performed with Quasar software 1.5.0 and full cross-validation (leave-one-out) was used. On the other hand, LDA was performed with JMP PRO 16.0.0 (SAS Institute Inc., 2018) and 6-fold cross-validation was used. Classification models were developed with raw spectra and with pre-processed spectra with the first derivative and SNV also applied in the PCA and PLS regressions. Moreover, the models were performed using the whole spectra (350–2500 nm), the Vis region (350–995 nm), the NIR region 1 (1005–1795 nm) and the NIR region 2 (1805–2500 nm), so 48 classification models for each type were developed. The models that classify the presence of specific fungi were based on 42 mean spectra of 14 different a_w/strain conditions (three replicates per condition) because only 0.98 and 0.90 a_w conditions were used. Samples incubated at a_w 0.80 were excluded from fungal classification models due to the absence of visible fungal growth and the lack of quantitative confirmation of fungal colonisation. Since inoculation alone does not guarantee fungal development under these low-moisture conditions, and no fungal biomass was measured, these samples could not be confidently classified as either positive or negative for fungal presence. To avoid mislabelling and model confusion, they were excluded from the analysis. Categories were created based on the presence of FL or non-presence of FL (NFL) and the presence of *Fusarium* T-2 and HT-2 toxins producers (P) or non-presence (NP). Meanwhile, for the development of classification models of the content of T-2 and HT-2 toxins we used the 60 mean spectra obtained. In these models, we created two categories according to whether oat samples were above (U) to the legal limit (1250 μg/kg) or below to this limit (L).

The evaluation parameters for classification models were classification accuracy, which represents the fraction of correctly categorised instances, and the confusion matrix, which includes true positive, true negative, false positive and false negative predictive rates. The best-fitted models were selected because they showed the closest to 100 classification accuracy and true positive and true negative predictive rates.

3. Results and discussion

3.1. Mycotoxins' content

Table 2 presents the concentration of mycotoxins in oat samples subjected to different fungal inoculation conditions under three a_w levels: 0.98, 0.90, and 0.80. The fungal species evaluated include FL, FS, FG, and FP. The mycotoxins analysed were T-2 toxin, HT-2 toxin, NIV, and DON, with total trichothecene content calculated as the sum of these toxins.

The results indicate that a_w of 0.98 favoured the highest mycotoxin production, suggesting that high moisture availability enhances fungal growth and secondary metabolism. The most affected mycotoxins were T-2 and HT-2 toxins, predominantly produced by FL and FS. We can also observe that FL1 was a higher producer of these mycotoxins than FL2, which may be since the former originated from the UK, while the latter was from Norway. FG was the main producer of DON, while FP was the only species contributing to NIV accumulation, although at significantly lower levels than the other trichothecenes. The total trichothecene content was the highest in FL and FS inoculated samples, confirming its strong toxigenic potential under optimal moisture conditions. Additionally, it is interesting to mention that when FP and FL2 are inoculated together, the production of mycotoxins by FL2 is significantly lower, especially at a_w of 0.98, possibly due to competition between these two fungi. This is an interesting finding, as these two fungi are commonly found together in oat crops (Xue et al., 2019).

A reduction in a_w to 0.90 significantly decreased mycotoxin production, indicating that moderate water restriction limits fungal

Table 2
Mycotoxins' content in oat samples with different fungal inoculation conditions (a_w of 0.98 and 0.90). *Fusarium langsethiae* (FL); *Fusarium sporotrichioides* (FS); *Fusarium graminearum* (FG); *Fusarium poae* (FP); deoxynivalenol (DON); nivalenol (NIV); limit of detection (LOD).

a_w	Fungi	Mycotoxin content (μg/kg)					
		T-2 toxin	HT-2 toxin	T-2 and HT-2 toxins	NIV	DON	Trichothecenes[a]
0.98	None (Control)	<LOD	<LOD	<LOD	<LOD	<LOD	<LOD
		<LOD	<LOD	<LOD	<LOD	<LOD	<LOD
		<LOD	<LOD	<LOD	30.0	<LOD	30.0
	FL1	709.3	513.1	1222.4	<LOD	<LOD	1222.4
		1705.2	749.2	2454.4	<LOD	<LOD	2454.4
		1157.7	797.6	1955.3	28.1	<LOD	1983.4
	FL2	606.3	415.3	1021.6	236.7	<LOD	1258.4
		814.9	546.1	1361.0	23.4	<LOD	1384.4
		911.9	518.8	1430.8	25.5	<LOD	1456.3
	FS	2739.3	1796.9	4536.2	<LOD	<LOD	4536.2
		2680.0	2576.6	5256.6	<LOD	<LOD	5256.6
		2634.7	1783.7	4418.4	<LOD	<LOD	4418.4
	FG	<LOD	<LOD	<LOD	<LOD	495.6	495.6
		<LOD	<LOD	<LOD	<LOD	607.5	607.5
		849.5	<LOD	849.5	<LOD	606.6	1456.0
	FP	<LOD	<LOD	<LOD	107.6	<LOD	107.6
		<LOD	<LOD	<LOD	90.0	<LOD	90.0
		<LOD	<LOD	<LOD	69.4	<LOD	69.4
	FL2 + FP	<LOD	<LOD	<LOD	63.3	<LOD	63.3
		<LOD	<LOD	<LOD	64.1	<LOD	64.1
		<LOD	<LOD	<LOD	63.1	<LOD	63.0
0.90	None (Control)	<LOD	<LOD	<LOD	<LOD	<LOD	<LOD
		<LOD	<LOD	<LOD	<LOD	<LOD	<LOD
		<LOD	191.7	191.7	<LOD	<LOD	191.7
	FL1	284.1	193.8	477.9	<LOD	<LOD	477.9
		<LOD	<LOD	<LOD	396.6	<LOD	396.6
		571.5	416.4	988.0	<LOD	<LOD	988.0
	FL2	<LOD	<LOD	<LOD	<LOD	<LOD	<LOD
		<LOD	<LOD	<LOD	77.9	<LOD	77.9
		<LOD	<LOD	<LOD	28.1	<LOD	28.1
	FS	568.0	<LOD	568.0	<LOD	<LOD	568.0
		564.9	<LOD	564.9	<LOD	<LOD	564.9
		<LOD	<LOD	<LOD	<LOD	<LOD	<LOD
	FG	<LOD	<LOD	<LOD	<LOD	<LOD	<LOD
		571.8	386.8	958.6	<LOD	<LOD	958.6
		<LOD	<LOD	<LOD	<LOD	<LOD	<LOD
	FP	<LOD	<LOD	<LOD	<LOD	<LOD	<LOD
		<LOD	<LOD	<LOD	<LOD	<LOD	<LOD
		<LOD	<LOD	<LOD	<LOD	<LOD	<LOD
	FL2 + FP	<LOD	<LOD	<LOD	<LOD	<LOD	<LOD
		<LOD	<LOD	<LOD	41.0	<LOD	41.0
		<LOD	<LOD	<LOD	160.0	<LOD	160.0

[a] Trichothecenes content is considered the sum of DON, NIV, T-2 and HT-2 toxins.

metabolism. While FL and FS still produce T-2 and HT-2 toxins, their concentrations were significantly lower than at a_w of 0.98. Similarly, FG exhibited a decline in DON production, and FP showed minimal NIV accumulation. The total trichothecene content in all samples decreased, highlighting that lower water availability reduces, but does not completely prevent, mycotoxin contamination.

At a a_w of 0.80 (data not shown), mycotoxin production was nearly suppressed, with most samples showing levels below the LOD for T-2 toxin, HT-2 toxin, DON, and NIV. This suggests that fungal growth and toxin biosynthesis were severely inhibited, likely preventing the fungi from reaching the metabolic state necessary for toxin production. That confirms the influence of environmental conditions (a_w) in mycotoxin production, a pattern that has been consistently observed in other studies (Kokkonen et al., 2012; Tekauz et al., 2008). The total trichothecene content was negligible across all fungal species, confirming that maintaining an a_w of 0.80 is an effective strategy for minimising trichothecene contamination in oats. These results highlight the critical role of moisture control in oat storage and processing to mitigate the risks associated with *Fusarium*-derived mycotoxins.

The results of this study align with previous research on the mycotoxin production by FL, FG, FP, and FS. FL was confirmed as one of the main producers of T-2 and HT-2 toxins, particularly at high moisture levels (a_w 0.98), which is consistent with previous findings (Edwards, 2009; Fredlund et al., 2013; Gil-Serna et al., 2022; Martin et al., 2018). Besides, FS contributed significantly to T-2 and HT-2 toxins production, consistent with Kokkonen et al. (2012) and Martin et al. (2018). Regarding FG, it was the major producer of DON with the highest concentrations found at a_w 0.98, as highlighted by Fredlund et al. (2013), Hietaniemi et al. (2016) and Martin et al. (2018). The correlation between FG infection and DON levels in our study further corroborates the established view that FG is the leading species responsible for DON contamination in cereals. In contrast, FP was primarily responsible for NIV production, which aligns with other authors (Edwards, 2009; Gil-Serna et al., 2022; Islam et al., 2021; Martin et al., 2018), who noted that FP predominantly produces NIV rather than T-2 toxin, HT-2 toxin or DON.

It is important to note that, although other trichothecenes (such as DON and NIV) were also analysed, their concentrations were substantially lower than those of T-2 and HT-2 toxins in all samples. Since none of the samples exceeded the EU maximum level for DON, and NIV levels remained consistently low, their impact on the spectral data was considered minimal. For this reason, the quantification and classification models for mycotoxins were developed exclusively for T-2 and HT-2 toxins, which were clearly the dominant toxins under the experimental conditions.

3.2. Comparison of spectral profiles

Fig. S1 presents twenty spectral profiles corresponding to the mean spectra of the three replicates for each a_w/strain condition studied. The primary spectral differences were observed in the Vis region, followed by the NIR region 1. When analysing the spectral profiles based on experimental conditions (Fig. S1a), variations were evident, although the major differences were concentrated in the Vis region. Regarding fungal strains (Fig. S1b), no clear distinctions were observed. Fig. S1c shows the spectral profiles categorised by a_w, where some overlap between different categories is also observed.

Fig. 1 illustrates seven spectral profiles corresponding to the mean spectra of each fungal species, independent of a_w. As in Fig. S1, the most pronounced differences occurred in the Vis region, indicating that fungal presence and metabolic activity influence the optical properties of oat grains. Each fungal species exhibited a distinct spectral signature (Fig. 1a), with the control samples showing the lowest reflectance and the most divergent profile. Notably, FL1 and FL2 exhibited similar spectral patterns, whereas samples inoculated with a combination of FL2, and FP displayed an intermediate spectral profile between those of FL2 and FP treated separately. In addition, spectral differences were observed between *Fusarium* species that are T-2 and HT-2 toxins producers (FL, FS, and the FL + FP combination) and non-producers (FP and FG) (Fig. 1b). Generally, the spectral profiles of toxin producers exhibited higher reflectance across the entire spectra.

The spectral profiles obtained in this study showed slight differences between *Fusarium* inoculated and non-inoculated oats, which is consistent with the findings of Teixido-Orries et al. (2023b). In this previous study, some overlap was observed in the NIR region (900–1700 nm) between oats contaminated with T-2 and HT-2 toxins at levels above and below 1000 μg/kg. However, Tekle et al. (2013) found that the spectral profiles of low-DON and high-DON oat ground samples were quite similar, but low-DON samples showed lower absorption in the Vis region and higher absorption in the NIR region compared to high-DON samples. Our study revealed similar patterns, with control oats showing lower reflectance in the NIR region compared to *Fusarium* toxin-producing oats. Our results are in line with Alisaac et al. (2019) who also observed higher spectral reflectance across the entire Vis-NIR spectrum in *Fusarium*-infected wheat kernels compared to non-infected kernels. Delwiche et al. (2011) reported significant Vis-NIR spectral differences between damaged and undamaged wheat kernels infected by *Fusarium*. The slight brownish discolouration in the hulls and caryopses of *Fusarium*-infected oats, a common symptom of *Fusarium* contamination that is difficult to detect with the human eye, is more noticeable in artificially contaminated oats and is likely a contributing factor to the spectral changes observed in the Vis region (Tekle et al., 2013).

3.3. PCAs

PCA was applied to the spectral data to explore the dataset, facilitating the identification of key patterns that relate to fungal contamination, a_w, and mycotoxin production in oat samples. The models were built using 42 mean spectra for analysing fungal presence and 60 mean spectra for evaluating both overall spectral data and the effect of a_w. These corresponded to 14 and 20 different a_w/fungal strains combinations, respectively, each tested in triplicate. To improve the accuracy and robustness of the models, two pre-treatment techniques were applied to the raw spectral data (first derivative and SNV).

The results of the PCA analysis clearly indicated that a_w was the most influential factor affecting the spectral profiles of the oat grains

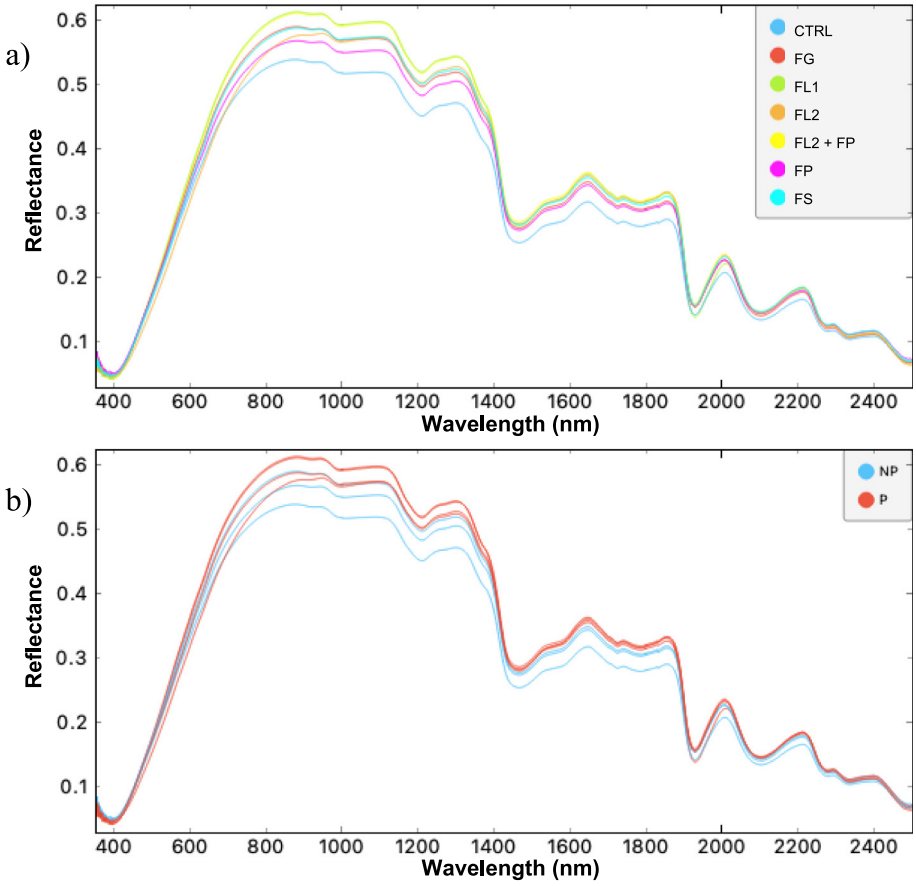


Fig. 1. Mean spectra profile of each type of fungi. a) Colour of the profiles by type of fungi. b) Colour of the profiles by Fusarium T-2 + HT-2 toxin producers (P) and non-producers (NP). Fusarium langsethiae (FL); Fusarium sporotrichioides (FS); Fusarium graminearum (FG); Fusarium poae (FP); Control (CTRL).

(Figs. S2, S3 and S4). In the PCA performed with raw spectra (Fig. S2) and first derivative pre-treatment (Fig. S3), a_w explained 15.0 % and 20.3 % of the variation in the data, respectively. The most notable differences were observed between the oat grains with high water activity (0.98), which were distinctly separated from the grains with 0.90 and 0.80 a_w. When SNV pre-treatment was applied, the results indicated that a_w was largely represented by the x-axis in the PCA plot, explaining nearly 80 % of the data variance. This finding further highlighted the dominant role of moisture content in differentiating the grains based on their spectral properties.

In contrast, the PCA analysis based on fungal type (as shown in Figs. S2a, S3a, and S4a) did not reveal clear clustering of the oat grains. This suggests that fungal species, such as *Fusarium* species, did not induce enough variation in the spectra to distinguish the grains effectively in a PCA (non-supervised method). Although the presence of *Fusarium* species, including FL, was expected to produce distinguishable spectral differences, the data indicated that fungal contamination alone was not the primary factor affecting the spectral characteristics of the oats. This finding suggests that while fungal type may influence the mycotoxin production, it does not directly correlate with easily detectable spectral changes in this context. A possible explanation is that the different *Fusarium* species may produce similar visual and structural symptoms in the oat grains, leading to overlapping spectral responses. Further analysis of the presence of FL (Figs. S2c, S3c and S4c) and T-2 and HT-2 toxins producers (Figs. S2d, S3d and S4d) also failed to reveal clear clustering in the PCA plots. This lack of clear classification may be due to overlapping spectral characteristics, which could reduce the sensitivity of the spectral data, making it insufficient to capture subtle differences.

The absence of clustering in the PCA based on fungal species and toxin producers led to the conclusion that supervised classification methods would be more effective for distinguishing between them. Therefore, supervised methods were recommended for further analysis. These approaches, which can model more complex relationships in the data, are better suited for classifying samples based on fungal contamination and mycotoxin production.

3.4. Quantification of T-2 and HT-2 toxins concentration in oat grains based on spectra

The objective was to develop models for the quantification of T-2 and HT-2 toxins in oat grains using spectral data. The models were based on 60 mean spectra, representing 20 different a_w/strain conditions, each with three replicates per condition. The spectral data was analysed across four regions: the Vis region, NIR region 1, NIR region 2, and the whole spectrum. The primary goal was to determine which spectral region provided the most accurate predictions for mycotoxin content in oats. Twelve PLS regressions models were performed and are presented in Table 3. The top four models were selected for RPD and wavelength analysis.

The Vis region provided the best results for the prediction of T-2 and HT-2 toxins concentrations (R^2 of 0.875 and 9 PCs), and was even superior to the whole spectrum (R^2 of 0.818 and 7 PCs), which included NIR regions that may have introduced noise into the models. In contrast, the NIR regions did not perform well for predicting the mycotoxins, with no clear fit described in any of the models for these spectral regions. This suggests that the Vis region contains the most relevant spectral information for the quantification of T-2 and HT-2 toxins, and its use may simplify the process by reducing the data needed without compromising accuracy. This may be since artificially contaminated oats are susceptible to darkening, a phenomenon that, although visually not distinguishable, is likely associated with the brownish discoloration in the hulls and caryopses commonly observed in *Fusarium*-infected oats by other authors (Tekle et al., 2013). This discoloration may contribute to differentiating between models by enhancing spectral distinctions in the Vis region.

For the whole spectrum, SNV was identified as the most effective pre-treatment. In the Vis region, although the models using raw data and SNV also yielded acceptable results, they generally performed slightly below those employing the first derivative pre-treatment.

The lowest value of RMSECV, which is a measure of the accuracy of the model, was obtained also from the model using the Vis region with first derivative pre-treatment. This model had an RMSECV of 394.65 μg/kg for T-2 and HT-2 toxins, indicating a good accuracy, although the EU legal limit is 1250 μg/kg. The RPD values confirm that the models developed for the Vis region with first derivative pre-treatment (2.83) and raw data (2.56) were able to provide accurate predictions for T-2 and HT-2 toxin concentrations in oats, with RPD values above 2.5, indicating a high performance.

In previous study, T-2 and HT-2 toxins levels were predicted in naturally contaminated oat samples using NIR-HSI, obtaining an R^2 of 0.64, an RMSECV of 157.80 μg/kg, and an RPD of 1.74 (Teixido-Orries et al., 2023b). Additionally, DON levels were predicted in naturally contaminated oat samples using the same device, achieving an R^2 of 0.85, an RMSECV of 312.64 μg/kg, and an RPD of 2.64 (Teixido-Orries et al., 2025a). The values of R^2 and RPD were worse than those obtained in this study, but RMSECV value was better, likely due to the use of naturally contaminated samples, different mycotoxin concentration distribution, the incorporation of HSI, and the fact that this study was conducted on individual grains. Moreover, Tekle et al. (2013) estimated DON content in ground artificially contaminated oats using Vis-NIR spectroscopy. Their best-fitted PLS regression model resulted in an RMSECV of 4060 μg/kg, an R^2 of 0.77, and an RPD of 2.09. This higher RMSECV value reported could be attributed to the broader range of mycotoxin concentrations analysed (0–30 mg/kg).

The analysis also highlighted that certain wavelength regions within the Vis spectra showed the highest correlation with T-2 and HT-2 toxins concentration. The regions with the highest regression coefficients were

Table 3
Performance parameters of T-2 and HT-2 toxins predictive cross-validated models for oat grains.

Spectral region	Pre-treatment	Validation parameters						
		Slope	Offset	RMSECV (μg/kg)	Correlation	R^2	SECV	PC
Whole spectra	Raw spectra	0.728	114.27	571.03	0.851	0.733	576.11	6
	1st derivative	0.677	119.14	583.24	0.845	0.722	588.01	6
	SNV	0.826	76.63	475.33	0.901	0.818	479.48	7
Vis region	Raw spectra	0.855	54.38	436.79	0.915	0.841	440.54	7
	1st derivative	0.842	58.35	394.65	0.934	0.875	397.87	9
	SNV	0.821	71.96	477.30	0.897	0.811	481.45	5
NIR region 1	Raw spectra	0.019	486.29	1116.69	0.082	0.019	1126.10	2
	1st derivative	0.021	468.58	1155.79	0.060	−0.050	1165.51	2
	SNV	0.063	460.99	1109.36	0.178	0.032	1119.72	1
NIR region 2	Raw spectra	0.000	490.48	1121.70	−0.002	0.011	1131.16	1
	1st derivative	0.003	475.92	1141.58	0.011	−0.025	1151.16	1
	SNV	0.058	460.07	1128.47	0.148	−0.001	1137.99	2

between 415 and 700 nm. This specific region was identified as the most relevant for predicting toxin content, and the models that utilised these wavelengths showed better performance. The key wavelengths contributing to the prediction of T-2 and HT-2 toxins were 464 nm, 568 nm, 575 nm and 636 nm. Interestingly, previous studies have reported similar findings. Tekle et al. (2013) found that the spectral wavelengths most effective for distinguishing between low-DON and high-DON oat ground samples were around 492 and 638 nm, along with the NIR range (1200–1850 nm). Similarly, Delwiche et al. (2011) identified significant spectral differences between *Fusarium*-damaged and undamaged wheat kernels at 502, 678, 1198, and 1498 nm using Vis-NIR HSI. Additionally, Barbedo et al. (2017) highlighted 623 and 1411 nm as key wavelengths for classifying DON content in wheat kernels with a similar device. These findings align with our results, particularly in the Vis region, reinforcing the relevance of these wavelengths for detecting mycotoxin contamination.

T-2 and HT-2 toxins in oats are present at much lower concentrations than the main grain components (starch, protein, water, etc.), making their direct detection by Vis-NIR spectroscopy challenging due to band overlap. Instead, the correlation between spectra and mycotoxins likely stems from the impact of *Fusarium* growth and toxin synthesis on the chemical and structural properties of oats. Although the specific relationship between chemical and physical changes and T-2 and HT-2 toxins contamination remains unclear, Martin et al. (2018) reported that FL infection altered β-glucan content. Besides, Tekle et al. (2013) observed a light darkening in some mycotoxin contaminated oats. However, visual symptoms not always imply a high content of mycotoxins. These structural and compositional changes may explain the ability of Vis-NIR spectroscopy to distinguish and quantify T-2 and HT-2 toxins in oat contaminated grains.

Despite the promising performance of the quantification models, their generalisability is currently limited by the relatively small and homogeneous dataset. A larger and more diverse sample set, including broader T-2 and HT-2 toxins concentration ranges, is essential to increase model robustness and predictive accuracy. This limitation is particularly relevant for Neural Network models, which are more prone to overfitting when trained on small datasets. Although leave-one-out cross-validation was applied to mitigate this risk, future work with larger and more diverse data is required to ensure more reliable and generalisable model performance. Furthermore, the spectral data may

Table 4
Validation accuracies and confusion matrix of oat grains discrimination best models according to the presence of *Fusarium langsethiae* (FL). lang. FL = presence of F. langsethiae; NFL = non-presence of F. langsethiae.

Spectral region	Pre-treatment	Model	Confusion matrix				Classification accuracy (%)
Whole spectra	None	Neural Network	Actual	Predicted rate (%)			76.2
					FL	NFL	
				FL	66.7	33.3	
				NFL	16.7	83.3	
	1st derivative	Neural Network	Actual	Predicted rate (%)			71.4
					FL	NFL	
				FL	61.1	38.9	
				NFL	20.8	79.2	
	SNV	Neural Network	Actual	Predicted rate (%)			73.8
					FL	NFL	
				FL	61.1	38.9	
				NFL	16.7	83.3	
Vis region	None	Neural Network	Actual	Predicted rate (%)			66.7
					FL	NFL	
				FL	55.6	44.4	
				NFL	25.0	75.0	
	1st derivative	Neural Network	Actual	Predicted rate (%)			71.4
					FL	NFL	
				FL	61.1	38.9	
				NFL	20.8	79.2	
	SNV	LDA	Actual	Predicted rate (%)			61.9
					FL	NFL	
				FL	55.5	44.5	
				NFL	33.3	66.7	
NIR region 1	None	Neural Network	Actual	Predicted rate (%)			57.1
					FL	NFL	
				FL	44.4	55.6	
				NFL	33.3	66.7	
	1st derivative	Neural Network	Actual	Predicted rate (%)			71.4
					FL	NFL	
				FL	66.7	33.3	
				NFL	25.0	75.0	
	SNV	Neural Network	Actual	Predicted rate (%)			69.0
					FL	NFL	
				FL	61.1	38.9	
				NFL	25.0	75.0	
NIR region 2	None	LDA	Actual	Predicted rate (%)			54.7
					FL	NFL	
				FL	50.0	50.0	
				NFL	41.7	58.3	
	1st derivative	LDA	Actual	Predicted rate (%)			54.7
					FL	NFL	
				FL	50.0	50.0	
				NFL	41.7	58.3	
	SNV	Neural Network	Actual	Predicted rate (%)			57.1
					FL	NFL	
				FL	50.0	50.0	
				NFL	37.5	62.5	

be subject to overlapping signals from other factors, which can influence the model's ability to isolate toxin-specific features. Future work should therefore include more complex datasets and validation with naturally contaminated grains to enhance model reliability under realistic scenarios.

3.5. Classification of oat grains regarding the presence of FL

Since FL is the major producer of T-2 and HT-2 toxins in the UK, classification models were developed to classify oat grains based on its presence (0.90 and 0.98 a_w). Best models for each spectral region and pre-treatment are showed in Table 4.

The Neural Network model applied to the whole spectra without any pre-treatment achieved the highest classification accuracy of 76.2 %, with a true positive rate of 66.7 % and a true negative rate of 83.3 %. This model was particularly effective in identifying non-inoculated grains, as evidenced by the high true negative rate, while also being capable of correctly identifying FL contamination, although there is still potential for improving the detection of all positive cases.

In addition to the best-performing model, several other models demonstrated good performance, achieving classification accuracy above 70 % and predicted rates >60 %. Notably, the whole spectrum + first derivative/SNV + Neural Network model and the Vis region/NIR region 1 + first derivative + Neural Network model also showed strong results. This reinforces the importance of selecting the appropriate pre-treatment method depending on the spectral region and classification model being used. These models indicate that the whole spectra can provide a comprehensive approach to FL detection, while the Vis region and NIR region 1 can still offer good alternatives when combined with appropriate pre-treatment methods. In contrast, the NIR region 2 did not show satisfactory results with any pre-treatment. This demonstrates that specific spectral regions can be highly useful for FL detection. Regarding classification models, Neural Network was the best overall model for identifying FL compared with LDA or kNN.

It is known that the Vis, particularly in orange and red bands (600–750 nm), is useful to detect FG or *F. culmorum* in wheat kernels only between mid-gran development and early grain remaining. In later stages of grain development, only NIR, especially in the 1000–1400 nm wavelength range, has the potential to detect the stresses caused by the disease (Barbedo et al., 2015). That fact could be the explanation of the Vis being the best region followed by NIR region 1. *Fusarium* damage assessment has been studied widely, but never the FL damage in oats. Tekle et al. (2015) classified with optimistic results individual pixels of oat artificially contaminated grains with NIR-HSI based on FG damage. Delwiche et al. (2011) classified wheat kernels according to FG damage using Vis-NIR HSI, achieving an average accuracy of approximately 95 %, a significantly higher result than ours, possibly due to the incorporation of HSI. Similarly, Barbedo et al. (2015) detected Fusarium Head Blight in wheat grains using HSI, obtaining a classification accuracy of 91 %. The lower classification accuracy observed in oats compared to wheat, may be attributed to several biological and structural factors. Unlike wheat, *Fusarium* infection in oats, particularly by FL, often remains asymptomatic, with minimal visible or structural changes to the grain surface, making optical detection more challenging. In addition, the presence of the outer hull in oats can obscure or attenuate the spectral signals associated with internal fungal activity, reducing the sensitivity of Vis-NIR measurements. These differences in infection visibility and grain anatomy likely contribute to the lower performance observed in this study.

These results suggest that while it is possible to detect FL in oats, further research and improvements in this field are needed to achieve higher classification accuracies because the classification of oat grains infected with FL also presents specific limitations. As no quantitative measurement of fungal growth was performed, the models were based solely on the presence or absence of visual growth after inoculation. This binary approach may not reflect varying levels of colonisation or infection intensity. Additionally, infections by FL are often asymptomatic, meaning that the spectral differences induced can be subtle and prone to overlap with those of healthy grains. This spectral similarity poses a challenge for accurate classification. Future research will aim to incorporate graded infection data and test classification models on naturally contaminated samples to improve sensitivity and specificity.

3.6. Classification of oat grains regarding the presence of Fusarium T-2 and HT-2 toxins producers

Besides, the classification of oat grains based on the presence of *Fusarium* T-2 and HT-2 toxins producers was carried out using the same methodology as in Section 3.5. The classification models aimed to differentiate between oat grains inoculated with *Fusarium* T-2 and HT-2 toxins producers (P) (FL, FS, and the FL + FP combination) and those without producers' inoculation (NP) (FP, FG and control). Best models for each spectral region and pre-treatment are showed in Table 5.

The top-performing model was the Neural Network model using the NIR region 1 with first derivative pre-treatment. This model achieved the highest classification accuracy of 71.4 %, with a true positive rate of 75.0 % and a true negative rate of 66.7 %. This indicates that the model was effective in identifying the *Fusarium* T-2 and HT-2 toxins producers, with good sensitivity for detecting contaminated grains and a reasonable specificity for non-contaminated grains. Other models demonstrate that different combinations of spectral regions and pre-treatment methods can also achieve acceptable classification accuracy. In particular, the Vis region provided acceptable results when used with first derivative pre-treatment in LDA, suggesting this region is also important for detecting *Fusarium* T-2 and HT-2 toxins producers. Additionally, the use of SNV pre-treatment in combination with the whole spectra also produced favourable results with Neural Network. Moreover, raw spectra models did not produce good results, underscoring the importance of applying the correct pre-treatment to the data to improve classification performance. Besides, NIR region 2 did not yield satisfactory results for the classification of *Fusarium* T-2 and HT-2 toxin producers, like its poor performance in Section 3.5.

The findings suggest that the NIR region 1 is the most useful spectral region for this application, although the whole spectrum and the Vis region can still offer useful. Other authors observed that the NIR region 1 is relevant for the prediction of *Fusarium* infection in individual oat grains and wheat kernels (Alisaac et al., 2019; Delwiche et al., 2011; Tekle et al., 2015). A recent study by Martin et al. (2018) showed that FL infection alters β-glucan levels, as well as protein content and grain weight. Besides, Yan et al. (2017) found that oat cultivars affected by *Fusarium* tend to have higher protein content and a greater hull (lower groat) percentage. Given that the NIR region is widely used for analysing chemical composition and moisture content (Walsh et al., 2020), these structural and compositional changes may explain why the NIR region 1 effectively predicts *Fusarium* presence in oats. However, the same study limitations as Section 3.5 are observed.

When comparing the results of this section with those of Section 3.5, it becomes clear that the classification accuracy of the best model for detecting *Fusarium* T-2 and HT-2 toxins producers (71.4 %) was slightly lower than the 76.2 % accuracy achieved for FL detection. However, the true positive rate values in this section were notably higher (75.0 %) compared to FL (66.7 %), indicating that while the classification of FL had a slightly higher overall accuracy, the classification of *Fusarium* HT-2 and T-2 toxins producers performed better in identifying positive samples.

3.7. Classification of oat grains according to T-2 and HT-2 toxins content

Oat grains were classified based on their T-2 and HT-2 toxins content, with two categories: T-2 and HT-2 toxins content above the EU limit (U) and below the EU limit (L). Best models for each spectral region and pre-treatment are presented in Table 6. These models are relevant

Table 5
Validation accuracies and confusion matrix of oat grains discrimination best models according to the presence of Fusarium T-2 and HT-2 toxins producers. P = Fusarium T-2 and HT-2 toxins producers; NP = non-presence of Fusarium T-2 and HT-2 toxins producers.

Spectral region	Pre-treatment	Model	Confusion matrix				Classification accuracy (%)
Whole spectra	None	Neural Network	Actual	Predicted rate (%)			66.7
					P	NP	
				P	75.0	25.0	
				NP	44.4	55.6	
	1st derivative	Neural Network	Actual	Predicted rate (%)			66.7
					P	NP	
				P	70.8	29.2	
				NP	38.9	61.1	
	SNV	Neural Network	Actual	Predicted rate (%)			69.0
					P	NP	
				P	70.8	29.2	
				NP	33.3	66.7	
Vis region	None	Neural Network	Actual	Predicted rate (%)			59.5
					P	NP	
				P	66.7	33.3	
				NP	50.0	50.0	
	1st derivative	LDA	Actual	Predicted rate (%)			69.0
					P	NP	
				P	66.7	33.3	
				NP	27.8	72.2	
	SNV	LDA	Actual	Predicted rate (%)			57.1
					P	NP	
				P	58.3	41.7	
				NP	33.3	66.7	
NIR region 1	None	Neural Network	Actual	Predicted rate (%)			61.9
					P	NP	
				P	66.7	33.3	
				NP	44.4	55.6	
	1st derivative	Neural Network	Actual	Predicted rate (%)			71.4
					P	NP	
				P	75.0	25.0	
				NP	33.3	66.7	
	SNV	LDA	Actual	Predicted rate (%)			69.0
					P	NP	
				P	70.8	29.2	
				NP	33.3	66.7	
NIR region 2	None	Neural Network	Actual	Predicted rate (%)			52.4
					P	NP	
				P	54.2	45.8	
				NP	50.0	50.0	
	1st derivative	Neural Network	Actual	Predicted rate (%)			69.0
					P	NP	
				P	75.0	25.0	
				NP	38.9	61.1	
	SNV	kNN	Actual	Predicted rate (%)			54.8
					P	NP	
				P	50.0	50.0	
				NP	38.9	61.1	

because ensuring the levels of these mycotoxins are within acceptable limits is crucial for food safety. It is important to note that classifying based on the presence of the mycotoxigenic fungi is not the same as categorising based on the presence of T-2 and HT-2 toxins, as the fungus may be present without necessarily producing these mycotoxins. The fungus can grow on the grain and induce changes that can be detected through spectroscopy, which may differ from the changes occurring when the fungus produces these toxins.

The best model was the LDA model applied to the Vis region with first derivative pre-treatment, which achieved the highest classification accuracy of 93.3 %. This model also showed excellent predicted rates, with 91.7 % for true positives and 94.0 % for true negatives, indicating that it was highly effective at classifying both contaminated and non-contaminated oat grains. That values make it a powerful tool for detecting T-2 and HT-2 toxins in oats. The best performance for the PLS prediction models (Section 3.4) was also achieved using these parameters.

Other models also showed promising results, with the whole spectra consistently performing well with LDA, while NIR region 1 performed adequately when combined with SNV and LDA. Moreover, raw spectra models generally showed slightly lower performance.

The good performance of the Vis region aligns with the findings from Sections 3.5 and 3.6, where it also performed well in classifying oats based on fungal contamination. This suggests that the Vis region is a particularly useful spectral region for detecting various contamination types in oats. Nevertheless, testing naturally contaminated oats is essential to validate these findings under real conditions, as natural contamination may present more variability and complexity than artificially inoculated samples. Besides, as also observed in previous sections, NIR region 2 was also not suitable for classifying mycotoxins content.

When comparing these results with those in Sections 3.5 and 3.6, classifying oat grains based on T-2 and HT-2 toxins content was more effective than classifying them based on the presence of FL or other *Fusarium* species capable of producing these toxins. Thus, it seems that the changes induced by mycotoxin production are more consistently detectable through spectral analysis than those resulting from fungal presence alone, which does not necessarily correlate with toxin production. This underscores the advantage of predicting mycotoxin content over fungal contamination, as the presence of mycotoxins directly

Table 6
Validation accuracies and confusion matrix of oat grains discrimination best models according to T-2 and HT-2 toxins content (threshold 1250 μg/kg). U = above the EU limit; L = below EU the limit.

Spectral region	Pre-treatment	Model	Confusion matrix				Classification accuracy (%)
Whole spectra	None	LDA	Actual	Predicted rate (%)			83.3
					U	L	
				U	66.7	33.3	
				L	13.9	86.1	
	1st derivative	LDA	Actual	Predicted rate (%)			85.0
					U	L	
				U	66.7	33.3	
				L	12.0	88.0	
	SNV	Neural Network	Actual	Predicted rate (%)			88.3
					U	L	
				U	55.6	44.4	
				L	5.9	94.1	
Vis region	None	LDA	Actual	Predicted rate (%)			86.7
					U	L	
				U	83.3	12.0	
				L	12.0	88.0	
	1st derivative	LDA	Actual	Predicted rate (%)			93.3
					U	L	
				U	91.7	8.3	
				L	6.0	94.0	
	SNV	LDA	Actual	Predicted rate (%)			93.3
					U	L	
				U	75.0	25.0	
				L	3.9	96.1	
NIR region 1	None	LDA	Actual	Predicted rate (%)			70.0
					U	L	
				U	58.3	41.7	
				L	27.5	72.5	
	1st derivative	LDA	Actual	Predicted rate (%)			75.0
					U	L	
				U	58.3	41.7	
				L	21.5	78.5	
	SNV	LDA	Actual	Predicted rate (%)			83.3
					U	L	
				U	75.0	25.0	
				L	13.9	86.1	
NIR region 2	None	Neural Network	Actual	Predicted rate (%)			81.7
					U	L	
				U	33.3	66.7	
				L	9.8	90.2	
	1st derivative	LDA	Actual	Predicted rate (%)			78.3
					U	L	
				U	25.0	75.0	
				L	12.3	87.7	
	SNV	Neural Network	Actual	Predicted rate (%)			81.7
					U	L	
				U	22.2	77.8	
				L	7.8	92.2	

relates to food safety risk. One likely reason for the lower accuracy of fungal classification models is that the mycotoxin models were trained using accurate quantitative data from chemical analysis, whereas fungal classification relied on binary labels based on visible growth. This lack of granularity regarding the extent of fungal colonisation may have limited model performance. In addition, fungal contamination does not always produce visible or measurable changes in the grain, particularly in the case of FL, which frequently infects oat grains asymptomatically. As a result, the spectral differences between infected and non-infected grains may have been too subtle or inconsistent to be reliably captured.

Furthermore, the fungal classification models excluded grains incubated at a_w 0.80 due to the absence of visible growth, whereas the toxin-based models included all a_w levels, thereby benefiting from a broader and more diverse dataset. These methodological differences may also have contributed to the lower classification performance observed for fungal detection.

When comparing with Section 3.4, it becomes evident that classification models may perform better than regression models in this case due to the nature of the data. In Section 3.4, the task was to predict the exact concentration of T-2 and HT-2 toxins in oats, which can be more challenging due to the continuous nature of the data, where many samples may have low or no contamination, while others have significantly higher toxin levels. In contrast, the classification models categorise samples into distinct groups (U and L), which simplifies the problem by reducing the complexity of the data. This dichotomy of low versus high contamination allows the classification models to work more efficiently, as the task becomes more about distinguishing between contaminated and non-contaminated samples, rather than predicting a precise concentration.

Moreover, while the results show promising performance, it is important to note that more grains and balanced categories are needed to further confirm and refine these results. Additionally, while the use of artificially inoculated oat grains allowed for controlled experimental conditions and clear identification of fungal species, it may not fully reflect the complexity of natural contamination scenarios, including environmental variability and co-infection by multiple *Fusarium* species. As such, the spectral patterns and toxin levels observed here may differ from those encountered in field-grown oats. To address this, future work will include validation of the developed models using naturally contaminated oat grains collected from commercial fields to improve

their robustness and real-world applicability. Therefore, the current models, while appropriate for an initial approximation, may be improved.

To our knowledge, no previous studies have classified individual oat grains based on T-2 and HT-2 content. However, in our previous research, oat naturally contaminated samples were classified according to DON, and T-2 and HT-2 toxins content, achieving maximum classification accuracies of 83.2 % and 94.1 %, respectively (Teixido-Orries et al., 2023b, 2023a). These values were comparable to those obtained in this study. The only classification models for single oat grains were developed by Tekle et al. (2015), who used NIR-HSI to classify individual pixels of oat artificially contaminated grains based on *Fusarium* damage and DON content. Their approach involved calculating the ratio of damaged pixels per kernel to differentiate between symptomatic categories and high/low DON levels. Their results demonstrated that NIR-HSI could detect grains with high DON content even if they appeared asymptomatic. Other studies have classified individual cereal kernels, such as wheat, for mycotoxin screening, achieving classification accuracies between 81 % and 83 % (Barbedo et al., 2017, 2015). If Vis-NIR spectroscopy is applied, it could potentially be a key strategy to reduce overall batch contamination, improve economic outcomes, and enhance the sustainability of the food industry. In this study, this approach has been demonstrated that could be possible in oats for detecting and removing grains contaminated with T-2 and HT-2 toxins.

4. Conclusions

As expected, based on known toxigenic profiles, FL and FS showed T-2 and HT-2 toxins production, while FG and FP were associated with DON and NIV production, respectively. The role of a_w in regulating mycotoxin production is evident, with higher a_w levels promoting increased toxin biosynthesis. These findings underline the importance of moisture control in reducing *Fusarium* contamination and mycotoxin risks in oats.

The application of Vis-NIR spectroscopy proved to be effective for both mycotoxin classification and *Fusarium* contamination detection in oats. The study shows that Vis-NIR spectroscopy can classify and quantify T-2 and HT-2 toxins in oats with a 93.3 % classification accuracy and a R^2 of 0.875. This direct detection of toxin levels provides a more relevant and reliable approach for food safety compared to fungal classification alone (which presented worse classification results).

Both the Vis region (350–995 nm) and NIR region 1 (1006–1795 nm) were identified as the most important spectral ranges for detecting FL and FS contamination, and trichothecenes type A in oats. This highlights the potential of Vis-NIR spectroscopy as a non-destructive, rapid, and cost-effective tool for mycotoxin detection and contamination monitoring in individual grains. Therefore, this study demonstrates that Vis-NIR spectroscopy can be employed for screening, sorting and removing heavily contaminated grains from oat batches, reducing mycotoxin levels.

Importantly, Vis-NIR spectroscopy has already been implemented in the agri-food industry for tasks such as detecting discoloured or damaged grains and analysing chemical composition in various products. As many commercial sorting systems already operate in the Vis and NIR ranges, integrating models like those developed in this study would not require major hardware modifications, making implementation technically feasible. Moreover, combining mycotoxin detection with existing quality control functions could maximise the return on investment. While detailed cost estimates were beyond the scope of this study, previous industrial applications suggest that Vis-NIR integration is economically viable, particularly in high-throughput processing environments where early detection can reduce downstream losses and health risks.

Although this study has shown promising results, further research with a high number of naturally contaminated individual grains is needed to refine the models and improve their robustness. This would broaden the applicability of Vis-NIR spectroscopy for mycotoxin detection and food safety monitoring in cereals and other agricultural products.

CRediT authorship contribution statement

Irene Teixido-Orries: Writing – original draft, Visualization, Validation, Software, Methodology, Investigation, Formal analysis, Data curation, Conceptualization. **Lexuan Yang:** Writing – original draft, Visualization, Validation, Software, Methodology, Investigation. **Francisco Molino:** Writing – review & editing, Writing – original draft, Supervision. **Angel Medina:** Supervision, Funding acquisition. **Sonia Marín:** Writing – review & editing, Writing – original draft, Supervision. **Carol Verheecke-Vaessen:** Writing – review & editing, Writing – original draft, Visualization, Validation, Supervision, Software, Methodology, Investigation, Funding acquisition, Data curation, Conceptualization.

Declaration of competing interest

The authors declare that they have no known competing financial interests or personal relationships that could have appeared to influence the work reported in this paper.

Acknowledgements

This research is supported by a BBSRC-SFI research grant (BB/P001432/1) between the Applied Mycology Group at Cranfield University and the School of Biology and Environmental Science, University College Dublin, Ireland. The article team thanks Prof. S. Edwards from Harper Adams University, Dr. I. S. Hofgaard from Norwegian Institute of Bioeconomy Research and Dr. P. Jennings from Food and Environment Research Agency Science Ltd., for providing the strains used in this study. The authors would like to thank Naresh MAGAN, Esther GARCIA-CELA, Toby WAINE, Fiona DOOHAN, Sofia KOURMPETLI, Sandra LANDAHL, Mari Carmen ALAMAR, Ian TRUCKELL, Daniel SIMMS and Amal KAHLA for their support in developing the methodology. This work was also supported by the Spanish Ministry of Universities (predoctoral grant FPU21/00073).

Appendix A. Supplementary data

Supplementary data to this article can be found online at https://doi.org/10.1016/j.ijfoodmicro.2025.111301.

Data availability

Data will be made available on request.

References

Agelet, L.E., Hurburgh, C.R., 2010. A tutorial on near infrared spectroscopy and its calibration. Crit. Rev. Anal. Chem. 40, 246–260. https://doi.org/10.1080/10408347.2010.515468.

Alisaac, E., Behmann, J., Rathgeb, A., Karlovsky, P., Dehne, H.W., Mahlein, A.K., 2019. Assessment of *Fusarium* infection and mycotoxin contamination of wheat kernels and flour using hyperspectral imaging. Toxins 11. https://doi.org/10.3390/toxins11100556.

Barbedo, J.G.A., Tibola, C.S., Fernandes, J.M.C., 2015. Detecting Fusarium head blight in wheat kernels using hyperspectral imaging. Biosyst Eng 131, 65–76. https://doi.org/10.1016/j.biosystemseng.2015.01.003.

Barbedo, J.G.A., Tibola, C.S., Lima, M.I.P., 2017. Deoxynivalenol screening in wheat kernels using hyperspectral imaging. Biosyst. Eng. 155, 24–32. https://doi.org/10.1016/j.biosystemseng.2016.12.004.

De Colli, L., De Ruyck, K., Abdallah, M.F., Finnan, J., Mullins, E., Kildea, S., Spink, J., Elliott, C., Danaher, M., 2021. Natural co-occurrence of multiple mycotoxins in unprocessed oats grown in Ireland with various production systems. Toxins 13. https://doi.org/10.3390/toxins13030188.

Delwiche, S.R., Kim, M.S., Dong, Y., 2011. *Fusarium* damage assessment in wheat kernels by Vis/NIR hyperspectral imaging. Sens. & Instrumen. Food Qual. 5, 63–71. https://doi.org/10.1007/s11694-011-9112-x.

Dropa, T., Dzuman, Z., Jonatova, P., 2021. Mycotoxins in oat flakes – changes during production and occurrence on the Czech market. Czech J. Food Sci. 39, 131–139. https://doi.org/10.17221/247/2020-CJFS.

Edwards, S.G., 2009. Fusarium mycotoxin content of UK organic and conventional oats. Food Addit. Contam. Part A Chem. Anal. Control Expo. Risk Assess. 26, 1063–1069. https://doi.org/10.1080/02652030902788953.

European Commission, 2013. Commission recommendation of 27 march 2013 on the presence of T-2 and HT-2 toxin in cereals and cereal products. Off. J. Eur. Union L. 12–15. https://doi.org/10.2903/j.efsa.2011.2481.

European Commission, 2023. Commission regulation (EU) 2023/915 of 25 April 2023 on maximum levels for certain contaminants in food and repealing Regulation (EC) No 1881/2006. Off. J. Eur. Union 119, 103–157.

European Commission, 2024a. Commission regulation (EU) 2024/1022 of 8 April 2024 amending regulation (EU) 2023/915 as regards maximum levels of deoxynivalenol in food. Off. J. Eur. Union L 1–4. https://doi.org/10.2903/j.efsa.2017.4718.

European Commission, 2024b. Commission regulation (EU) 2024/1038 of 9 April 2024 amending regulation (EU) 2023/915 as regards maximum levels of T-2 and HT-2 toxins in food. Official Journal of the European Union L 1–5. https://doi.org/10.2903/j.efsa.2011.2481.

FAOSTAT Food and Agriculture Organization of the United Nations, 2023. FAOSTAT. http://www.fao.org/faostat/en/#data/QC. Accessed: 12-Feb-2025.

Femenias, A., Gatius, F., Ramos, A.J., Sanchis, V., Marín, S., 2020. Use of hyperspectral imaging as a tool for *Fusarium* and deoxynivalenol risk management in cereals: a review. Food Control. https://doi.org/10.1016/j.foodcont.2019.106819.

Fredlund, E., Gidlund, A., Sulyok, M., Börjesson, T., Krska, R., Olsen, M., Lindblad, M., 2013. Deoxynivalenol and other selected fusarium toxins in Swedish oats - occurrence and correlation to specific *Fusarium* species. Int. J. Food Microbiol. 167, 276–283. https://doi.org/10.1016/j.ijfoodmicro.2013.06.026.

Gil-Serna, J., Patiño, B., Verheecke-Vaessen, C., Vázquez, C., Medina, Á., 2022. Searching for the *Fusarium* spp. which are responsible for trichothecene contamination in oats using metataxonomy to compare the distribution of toxigenic species in fields from Spain and the UK. Toxins 14. https://doi.org/10.3390/toxins14090592.

Hietaniemi, V., Rämö, S., Yli-Mattila, T., Jestoi, M., Peltonen, S., Kartio, M., Sieviläinen, E., Koivisto, T., Parikka, P., 2016. Updated survey of *Fusarium* species and toxins in Finnish cereal grains. Food Addit. Contam. Part A Chem. Anal. Control Expo. Risk Assess. 33, 831–848. https://doi.org/10.1080/19440049.2016.1162112.

Islam, M.N., Tabassum, M., Banik, M., Daayf, F., Dilantha Fernando, W.G., Harris, L.J., Sura, S., Wang, X., 2021. Naturally occurring *Fusarium* species and mycotoxins in oat grains from Manitoba, Canada. Toxins 13. https://doi.org/10.3390/toxins13090670.

Janik, E., Niemcewicz, M., Podogrocki, M., Ceremuga, M., Stela, M., Bijak, M., 2021. T-2 toxin—the most toxic trichothecene mycotoxin: metabolism, toxicity, and decontamination strategies. Molecules. https://doi.org/10.3390/molecules26226868.

Kokkonen, M., Medina, A., Magan, N., 2012. Comparative study of water and temperature relations of growth and T-2/HT-2 toxin production by strains of *Fusarium sporotrichioides* and *Fusarium langsethiae*. World Mycotoxin J 5, 365–372. https://doi.org/10.3920/WMJ2012.1406.

Kolawole, O., De Ruyck, K., Greer, B., Meneely, J., Doohan, F., Danaher, M., Elliott, C., 2021. Agronomic factors influencing the scale of *Fusarium* mycotoxin contamination of oats. Journal of Fungi 7. https://doi.org/10.3390/jof7110965.

Luo, S., Du, H., Kebede, H., Liu, Y., Xing, F., 2021. Contamination status of major mycotoxins in agricultural product and food stuff in Europe. Food Control. https://doi.org/10.1016/j.foodcont.2021.108120.

Malachová, A., Sulyok, M., Beltrán, E., Berthiller, F., Krska, R., 2014. Optimization and validation of a quantitative liquid chromatography-tandem mass spectrometric method covering 295 bacterial and fungal metabolites including all regulated mycotoxins in four model food matrices. J. Chromatogr. A 1362, 145–156. https://doi.org/10.1016/j.chroma.2014.08.037.

Marin, S., Ramos, A.J., Cano-Sancho, G., Sanchis, V., 2013. Mycotoxins: occurrence, toxicology, and exposure assessment. Food Chem. Toxicol. https://doi.org/10.1016/j.fct.2013.07.047.

Martin, C., Schöneberg, T., Vogelgsang, S., Mendes Ferreira, C.S., Morisoli, R., Bertossa, M., Bucheli, T.D., Mauch-Mani, B., Mascher, F., 2018. Responses of oat grains to *Fusarium poae* and *F. langsethiae* infections and mycotoxin contaminations. Toxins 10. https://doi.org/10.3390/toxins10010047.

Perkowski, J., Stuper, K., Buśko, M., Góral, T., Jeleń, H., Wiwart, M., Suchowilska, E., 2012. A comparison of contents of group A and B trichothecenes and microbial counts in different cereal species. Food Addit. Contam. Part B Surveill. 5, 151–159. https://doi.org/10.1080/19393210.2012.675591.

Pettersson, H., 2011. Toxicity and risks with T-2 and HT-2 toxins in cereals. Plant Breeding and Seed Science 64. https://doi.org/10.2478/v10129-011-0029-7.

Rasane, P., Jha, A., Sabikhi, L., Kumar, A., Unnikrishnan, V.S., 2015. Nutritional advantages of oats and opportunities for its processing as value added foods - a review. J. Food Sci. Technol. https://doi.org/10.1007/s13197-013-1072-1.

Rossi, V., Giosuè, S., Terzi, V., Scudellari, D., 2007. A decision support system for Fusarium head blight on small grain cereals. EPPO Bulletin 37, 359–367. https://doi.org/10.1111/j.1365-2338.2007.01138.x.

Teixido-Orries, I., Molino, F., Femenias, A., Ramos, A.J., Marín, S., 2023a. Quantification and classification of deoxynivalenol-contaminated oat samples by near-infrared hyperspectral imaging. Food Chem., 135924 https://doi.org/10.1016/j.foodchem.2023.135924.

Teixido-Orries, I., Molino, F., Gatius, F., Sanchis, V., Marín, S., 2023b. Near-infrared hyperspectral imaging as a novel approach for T-2 and HT-2 toxins estimation in oat samples. Food Control 153. https://doi.org/10.1016/j.foodcont.2023.109952.

Teixido-Orries, I., Molino, F., Castro-Criado, B., Jodkowska, M., Medina, A., Marín, S., Verheecke-Vaessen, C., 2025a. Mapping variability of mycotoxins in individual oat kernels from batch samples: implications for sampling and food safety. Toxins 17. https://doi.org/10.3390/toxins17010034.

Teixido-Orries, I., Molino, F., Pascari, X., Ramos, A.J., Marín, S., 2025b. Impact of processing parameters and formulation on deoxynivalenol content and transfer in oat-based beverage manufacturing. LWT 218. https://doi.org/10.1016/j.lwt.2025.117368.

Tekauz, A., Fetch, J.W.M., Rossnagel, B.G., Savard, M.E., 2008. Progress in assessing the impact of fusarium head blight on oat in western Canada and screening of avena germplasm for resistance. Cereal Res. Commun. 49–56. https://doi.org/10.1556/CRC.36.2008.Suppl.B.8.

Tekle, S., Bjørnstad, Å., Skinnes, H., Dong, Y., Segtnan, V.H., 2013. Estimating deoxynivalenol content of ground oats using VIS-NIR spectroscopy. Cereal Chem 90, 181–185. https://doi.org/10.1094/CCHEM-07-12-0084-R.

Tekle, S., Mage, I., Segtnan, V.H., Bjornstad, A., 2015. Near-infrared hyperspectral imaging of *Fusarium*-damaged oats (*Avena sativa* L.). Cereal Chem. 92, 73–80. https://doi.org/10.1094/CCHEM-04-14-0074-R.

Thies, F., Masson, L.F., Boffetta, P., Kris-Etherton, P., 2014. Oats and CVD risk markers: a systematic literature review. Br. J. Nutr. https://doi.org/10.1017/S0007114514002281.

Tittlemier, S.A., Blagden, R., Chan, J., McMillan, T.L., Pleskach, K., Izydorczyk, M.S., 2020. Effects of processing whole oats on the analysis and fate of mycotoxins and ergosterol. World Mycotoxin J. 13, 45–56. https://doi.org/10.3920/WMJ2019.2530.

Toplak, M., Read, S.T., Sandt, C., Borondics, F., 2021. Quasar: easy machine learning for biospectroscopy. Cells 10. https://doi.org/10.3390/cells10092300.

Verheecke-Vaessen, C., Diez-Gutierrez, L., Renaud, J., Sumarah, M., Medina, A., Magan, N., 2019. Interacting climate change environmental factors effects on *Fusarium langsethiae* growth, expression of Tri genes and T-2/HT-2 mycotoxin production on oat-based media and in stored oats. Fungal Biol. 123, 618–624. https://doi.org/10.1016/j.funbio.2019.04.008.

Walsh, K.B., Blasco, J., Zude-Sasse, M., Sun, X., 2020. Visible-NIR 'point' spectroscopy in postharvest fruit and vegetable assessment: the science behind three decades of commercial use. Postharvest Biol. Technol. https://doi.org/10.1016/j.postharvbio.2020.111246.

Xue, A.G., Chen, Y., Seifert, K., Guo, W., Blackwell, B.A., Harris, L.J., Overy, D.P., 2019. Prevalence of *Fusarium* species causing head blight of spring wheat, barley and oat in Ontario during 2001–2017. Can. J. Plant Pathol. 41, 392–402. https://doi.org/10.1080/07060661.2019.1582560.

Yan, W., Pageau, D., Martin, R., Cummiskey, A., Blackwell, B., 2017. Is deoxynivalenol contamination a serious problem for oat in eastern Canada? Crop. Sci. 57, 88–98. https://doi.org/10.2135/cropsci2016.04.0263.



https://dspace.org/

Detection of Fusarium spp. and T-2 and HT-2 toxins contamination in oats using visible and near-infrared spectroscopy

Teixido-Orries, Irene; Yang, Lexuan; Molino, Francisco; Medina, Angel; Marín, Sonia ...

2025-10-02
Elsevier
https://doi.org/10.1016/j.ijfoodmicro.2025.111301
Teixido-Orries I, Yang L, Molino F, et al., (2025) Detection of Fusarium spp. and T-2 and HT-2 toxins contamination in oats using visible and near-infrared spectroscopy. International Journal of Food Microbiology, Volume 441, October 2025, Article number 111301

Downloaded from a DSpace repository. https://dspace.org/